

RSC Advances

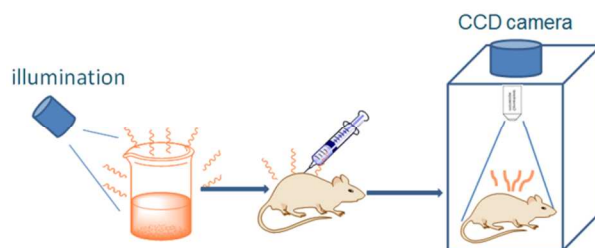


This is an *Accepted Manuscript*, which has been through the Royal Society of Chemistry peer review process and has been accepted for publication.

Accepted Manuscripts are published online shortly after acceptance, before technical editing, formatting and proof reading. Using this free service, authors can make their results available to the community, in citable form, before we publish the edited article. This *Accepted Manuscript* will be replaced by the edited, formatted and paginated article as soon as this is available.

You can find more information about *Accepted Manuscripts* in the [Information for Authors](#).

Please note that technical editing may introduce minor changes to the text and/or graphics, which may alter content. The journal's standard [Terms & Conditions](#) and the [Ethical guidelines](#) still apply. In no event shall the Royal Society of Chemistry be held responsible for any errors or omissions in this *Accepted Manuscript* or any consequences arising from the use of any information it contains.



$\beta\text{-Ga}_2\text{O}_3\text{:Cr}^{3+}$ nanorod can last its near infrared signal after the removal of exciting UV, and this afterglow can be acquired by CCD camera without external light source.

COMMUNICATION

Multi-functional mesoporous $\beta\text{-Ga}_2\text{O}_3\text{:Cr}^{3+}$ nanorod with long lasting near infrared luminescence for *in vivo* imaging and drug delivery

Cite this: DOI: 10.1039/x0xx00000x

Received 00th January 2012,
Accepted 00th January 2012

DOI: 10.1039/x0xx00000x

www.rsc.org/

Xin-Shi Wang^a, Wei-Shuo Li^a, Jun-Qing Situ^a, Xiao-Ying Ying^a, Hui Chen^a, Yi-Jin^{*b}, Yong-Zhong Du^{*a}

The long lasting luminescent $\beta\text{-Ga}_2\text{O}_3\text{:Cr}^{3+}$ nanorod allows detection in rather deep organs hours after injection based on the fact that it exhibits more than 72 h afterglow in the wavelength range of 650–850nm after ceasing the ultraviolet light irradiation. Besides, its mesoporous structure provides a reservoir for anticancer drugs.

As the developments of sensitive optical sensors and powerful probes such as semiconductor nanocrystals^{1–4}, fluorescent proteins^{5,6}, or near-infrared fluorescent molecules^{7–9}, optical imaging is an emerging tool for *in vivo* studies. However, it faces numerous disadvantages. The first one is the auto-fluorescence¹⁰ from tissue organic resulting in poor signal-to-noise ratio. In addition, deep tissue imaging is difficult because of intrinsic tissue signal attenuation.

Multi-functional nanoparticles combining imaging with drug delivery are developed to improve the outcome of drug therapy. Notably, these multi-functional drug deliveries usually consist of more than one component, combined physically or chemically. However, in the fabrication of a multi-component composite nanosystem^{11,12}, the multistep synthetic procedures and sometimes stringent synthetic conditions are involved. Some toxic surfactants or solvents are employed into the reaction system, which limits the application of final material with significant toxicity¹³. Besides, a composite structure commonly results in the performance degradation of individual component and inhomogeneity of the morphology and properties of the constructed system¹².

To address these difficulties above, we developed a uniform, mesoporous, nano-scale $\beta\text{-Ga}_2\text{O}_3\text{:Cr}^{3+}$ with a universal and convenient method. The $\beta\text{-Ga}_2\text{O}_3\text{:Cr}^{3+}$ nanorod can be optically excited before *in vivo* local or systemic injection and its long-lasting afterglow can eliminate the background noise originating from *in situ* excitation. Also, the mesoporous nature of $\beta\text{-Ga}_2\text{O}_3\text{:Cr}^{3+}$ was firstly exploited to serve as a reservoir for anticancer drug storage and controlled drug release.

The $\beta\text{-Ga}_2\text{O}_3\text{:Cr}^{3+}$ nanorod was synthesized by the hydrothermal process followed by calcination. The GaOOH:Cr^{3+} was firstly synthesized through the improved hydrothermal process in which not only reaction temperature and time were decreased, but also PEG400 was employed as a template to orient attachment of the GaOOH:Cr^{3+} . After a calcination of the obtained GaOOH:Cr^{3+} , the mesoporous $\beta\text{-Ga}_2\text{O}_3\text{:Cr}^{3+}$ nanorod was synthesized. The structure of the

GaOOH:Cr^{3+} was confirmed by the XRD (Fig. S1A, ESI†) and the transmission electron microscope (TEM) image of the GaOOH:Cr^{3+} (Fig. 1A) showed a rod-like shape with approximately 500nm length and 250nm width whose hydrodynamic diameter was measured at $360\pm 87\text{nm}$ (Fig. S2, ESI†). Notably, the calcination after which the GaOOH:Cr^{3+} transformed into $\beta\text{-Ga}_2\text{O}_3\text{:Cr}^{3+}$, imparted the $\beta\text{-Ga}_2\text{O}_3\text{:Cr}^{3+}$ with a mesoporous structure (Fig. 1B) without any changes to its original shape and size (Fig. 1B) which provided a possibility for the final $\beta\text{-Ga}_2\text{O}_3\text{:Cr}^{3+}$ to be applied *in vivo*.

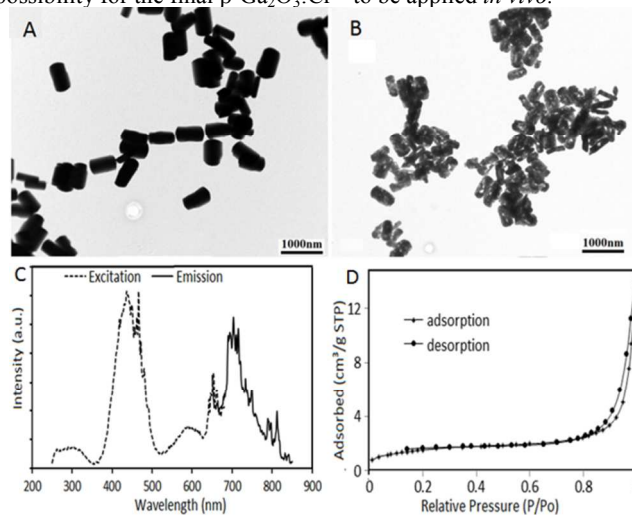


Fig. 1. TEM images of GaOOH:Cr^{3+} (A) and $\beta\text{-Ga}_2\text{O}_3\text{:Cr}^{3+}$ (B); (C) Excitation spectrum and emission spectrum of $\beta\text{-Ga}_2\text{O}_3\text{:Cr}^{3+}$ nanorod; (D) Nitrogen adsorption-desorption isotherm of mesoporous $\beta\text{-Ga}_2\text{O}_3\text{:Cr}^{3+}$.

Similarly, $\beta\text{-Ga}_2\text{O}_3\text{:Cr}^{3+}$ was confirmed by the XRD (Fig. S1B, ESI†). The weight content of Cr^{3+} doped in $\beta\text{-Ga}_2\text{O}_3$ was 0.24 % (Fig. S3, ESI†) and there was a weight loss during the conversion from GaOOH:Cr^{3+} to $\beta\text{-Ga}_2\text{O}_3\text{:Cr}^{3+}$, at 14.05 % (Fig. S4, ESI†) analyzed by thermogravimetry. The excitation spectrum and emission spectrum of $\beta\text{-Ga}_2\text{O}_3\text{:Cr}^{3+}$ nanorod were shown in Fig. 1C. The emission spectrum band was quite large (650–850 nm) in the near infrared scope. The mesoporous structure of the $\beta\text{-Ga}_2\text{O}_3\text{:Cr}^{3+}$

was confirmed by nitrogen adsorption-desorption isotherm (Fig. 1D). The isotherm can be classified as a type IV, which is the characteristic of mesoporous structure.

To investigate the long lasting near infrared luminescence of the synthesized $\beta\text{-Ga}_2\text{O}_3\text{:Cr}^{3+}$, the nanorod was excited by UV. Subsequently the long lasting luminescence signal was collected by *in vivo* imaging system after ceasing the UV. As shown in Fig. 2, the persistent near infrared luminescence of the nanorod could be detected even at 72 h post-excitation, and also the material could be excited repeatedly with the same emission intensity.

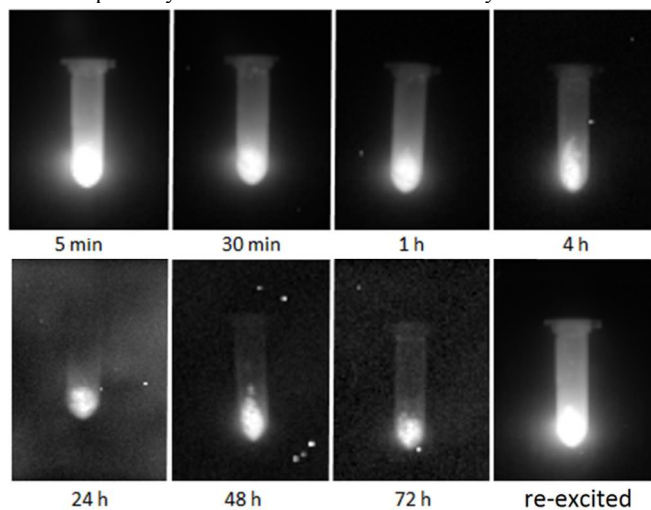


Fig. 2. Time dependence of the luminescence intensity of the $\beta\text{-Ga}_2\text{O}_3\text{:Cr}^{3+}$ nanorods and afterglow image of $\beta\text{-Ga}_2\text{O}_3\text{:Cr}^{3+}$ which was re-excited with white light.

In order to study the cytotoxicity of $\beta\text{-Ga}_2\text{O}_3\text{:Cr}^{3+}$ nanorod, Cell Counting Kit (CCK8) assay was performed on L929 and MCF-7 cell lines. As shown in Fig. 3A, the viabilities of the two kinds of cells were all above 85 % when the concentration of $\beta\text{-Ga}_2\text{O}_3\text{:Cr}^{3+}$ reached 800 $\mu\text{g/ml}$.

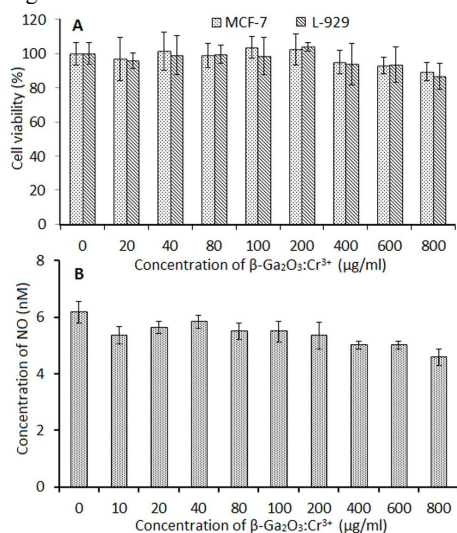


Fig. 3. (A) The viabilities of L-929 and MCF-7 cells incubated with a serial of concentrations of $\beta\text{-Ga}_2\text{O}_3\text{:Cr}^{3+}$ nanorod for 24h; (B) The concentration of NO after RAW 264.7 exposed to a serial of concentrations of $\beta\text{-Ga}_2\text{O}_3\text{:Cr}^{3+}$ nanorod for 24h.

Furthermore, the different levels of Nitric oxide (NO, which is one of the pro-inflammatory mediators produced by macrophages, playing an important role in patho-physiological responses including

inflammation¹⁴, infection¹⁵ and neurodegenerative disorders¹⁶) produced by macrophage RAW 264.7 cells after exposed to different concentrations of $\beta\text{-Ga}_2\text{O}_3\text{:Cr}^{3+}$ nanorod were detected. Fig. 3B showed that the levels of NO had no significant changes among all the treatment groups, nearly the same as the control group which presented another testify for the low toxicity and considerable biocompatibility of the $\beta\text{-Ga}_2\text{O}_3\text{:Cr}^{3+}$ nanorod.

The persistent near-infrared luminescence of the $\beta\text{-Ga}_2\text{O}_3\text{:Cr}^{3+}$ nanorod *in vivo* was further studied. After being exposed to UV for 3 min, the suspension of $\beta\text{-Ga}_2\text{O}_3\text{:Cr}^{3+}$ nanorod was subcutaneously injected into three different locations on the back of the mouse at different doses (from up to bottom: 300 μg , 200 μg , 100 μg). As shown in Fig. 4A, the afterglow of $\beta\text{-Ga}_2\text{O}_3\text{:Cr}^{3+}$ nanorods at different doses was observed at 1 h post-injection (exposure time: 2 min) and the intensity of the signal increased with the increase of dose. However, when the nude mouse was exposed to the *in vivo* imaging system under fluorescence mode, the auto-fluorescence of the nude mouse was so strong that it severely interfered the targeted fluorescence (Fig. S5, ESI†) which testified the superiority of the afterglow in bio-imaging.

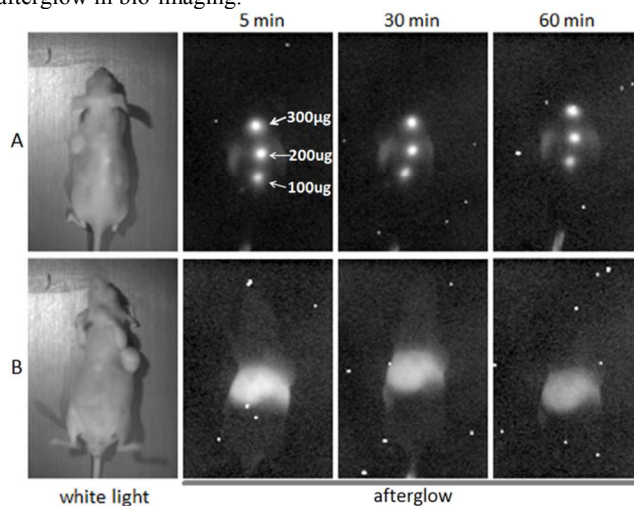


Fig. 4. *In vivo* near infrared persistent luminescence images acquired by *in-vivo* imaging system after a subcutaneous injection (A) and intravenous injection (B).

To testify whether the near infrared afterglow signal in the deep tissue can be easily monitored or not, the suspension of $\beta\text{-Ga}_2\text{O}_3\text{:Cr}^{3+}$ nanorod was intravenously injected. As shown in Fig. 4B, at 1 h-post *i. v.* injection, the $\beta\text{-Ga}_2\text{O}_3\text{:Cr}^{3+}$ was mainly accumulated in the liver resulting in an intense afterglow and at 48 h-post *i. v.* injection, as a result of EPR effect, the $\beta\text{-Ga}_2\text{O}_3\text{:Cr}^{3+}$ gradually accumulated into the tumour and an afterglow signal was observed in the tumour from the result of the *ex vivo* imaging (Fig. 5).

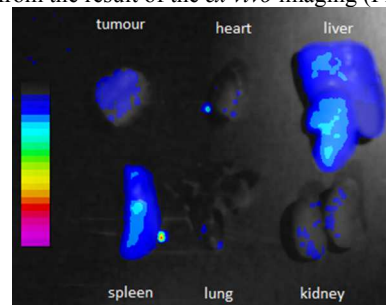


Fig. 5. Afterglow image of the isolated organs and tumour from a mouse bearing HeLa tumour at 48 h post- *i. v.* injection of $\beta\text{-Ga}_2\text{O}_3\text{:Cr}^{3+}$ which was re-excited by white light.

To investigate the potential of the mesoporous $\beta\text{-Ga}_2\text{O}_3\text{:Cr}^{3+}$ nanorod as a drug reservoir, DOX, which was a model anticancer drug, was chosen to evaluate drug loading rate and release kinetics. After stirring with DOX solution in PBS for 12 h, DOX loaded $\beta\text{-Ga}_2\text{O}_3\text{:Cr}^{3+}$ nanorod was collected by centrifugation followed by washing with PBS. The loading rate was 8.0 %. The burst and sustained release kinetics of DOX from $\beta\text{-Ga}_2\text{O}_3\text{:Cr}^{3+}$ nanorod were shown in Fig. 6A. The profiles clearly showed that the pH of the medium had a strong effect on the DOX release rate from the $\beta\text{-Ga}_2\text{O}_3\text{:Cr}^{3+}$ nanorod. The DOX release rate in pH 5.5 was higher than that in pH 7.4, which demonstrated that in the physiological environment, DOX released slowly from the nanorod. When the nanorod was up taken by the tumour cells, the intracellular acidic environment would accelerate the drug release.

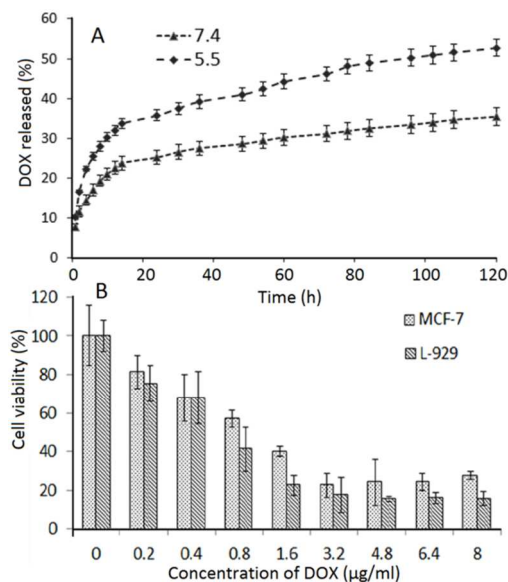


Fig. 6 (A) Release profiles of DOX from $\beta\text{-Ga}_2\text{O}_3\text{:Cr}^{3+}$ nanorod under different pH. (B) The vibrations of cells viabilities against DOX-loaded $\beta\text{-Ga}_2\text{O}_3\text{:Cr}^{3+}$ nanorod concentrations

Pharmacological effect of the drug loaded nanorod against L929 and MCF-7 cells was assessed by CCK-8 assay. As shown in Fig. 6B, the cytotoxicity of DOX loaded $\beta\text{-Ga}_2\text{O}_3\text{:Cr}^{3+}$ nanorod was significantly improved compared with the blank $\beta\text{-Ga}_2\text{O}_3\text{:Cr}^{3+}$ nanorod (Fig.3A). This may be explained by that DOX was released from the carriers to kill the tumour cells.

Conclusions

In summary, uniform and nano-sized $\beta\text{-Ga}_2\text{O}_3\text{:Cr}^{3+}$ was synthesized via a convenient and ground-saving method. The long lasting luminescent $\beta\text{-Ga}_2\text{O}_3\text{:Cr}^{3+}$ nanorod allowed detection in rather deep organs hours after injection. Besides, its mesoporous structure provided a reservoir for anticancer drugs and could realize a pH dependent drug release. The nano-sized mesoporous $\beta\text{-Ga}_2\text{O}_3\text{:Cr}^{3+}$ we fabricated was full of potential as a multifunctional drug delivery.

This work was supported by the Scientific Research Fund of Ministry of Health - Medical Science Major Technology Fund Project of Zhejiang Province (No. WKJ2012-2-023), National Nature Science Foundation of China (NO. 81373345), and the Nature Science Foundation of Zhejiang province (NO. LZ13H300001).

Notes and references

a. College of Pharmaceutical Sciences, Zhejiang University, 866Yuhangtang Road, Hangzhou 310058, P.R. China

b. National Pharmaceutical Engineering Center for Solid Preparation in Chinese Herbal Medicine, Jiangxi University of Traditional Chinese Medicine, Nanchang 56 Yangming Road, 330006, P.R. China

* Corresponding author: Tel: +86 571 88208439; Fax: +86 571 88208439.

E-mail address: duyongzhong@zju.edu.cn (Y.Z. Du); jinyizju@hotmail.com (Y. Jin)

Electronic supplementary information (ESI) available: Detailed Experimental, XRD, Size distribution and TGA of GaOOH:Cr^{3+} ; XRD and EDS of $\beta\text{-Ga}_2\text{O}_3\text{:Cr}^{3+}$; Bioimaging of nude mouse with $\beta\text{-Ga}_2\text{O}_3\text{:Cr}^{3+}$ fluorescence. See DOI:

- 1 X. Michalet, F. F. Pinaud, L. A. Bentolila, J. M. Tsay, S. Doose, J. J. Li, G. Sundaresan, A. M. Wu, S. S. Gambhir and S. Weiss, *Science*, 2005, **307**, 538.
- 2 B. Dubertret, P. Skourides, D. J. Noriis, V. Noireaux, A. H. Brivanlou and A. Libchader, *Science*, 2002, **298**, 1759.
- 3 M. K. So, C. Xu, A. M. Loening, S. S. Gambhir and J. Rao, *Nat Biotech*, 2006, **24**, 339.
- 4 B. Ballou, B. C. Lagerholm, L. A. Ernst, M. P. Bruchez and A. S. Waggoner, *Bioconjugate Chem*, 2004, **15**, 79.
- 5 S. Bhaumik and S. S. Gambhir, *Proc Natl Acad Sci USA*, 2002, **99**, 377.
- 6 C. H. Contag and M. H. Bachmann, *Annu Rev Biomed Eng*. 2002, **4**, 235.
- 7 Z. Cheng, J. Levi, Z. Xiong, O. Gheysens, S. Keren, X. Chen and S. S. Gambhir, *Bioconjugate Chem*, 2006, **17**, 662.
- 8 R. Weissleder, C. H. Tung, U. Mahmood and A. Bogdanov, *Nat Biotechnol*, 1999, **17**, 375.
- 9 A. Becker, C. Hessenius, K. Licha, B. Ebert, U. Sukowski, W. Semmler, B. Wiedenmann and C. Grotzinger, *Nat Biotechnol*, 2001, **19**, 327.
- 10 J. V. Frangioni, *Current Opin Chem Bio*. 2003, **7**, 626.
- 11 D. Shi, H. Cho, Y. Chen, H. Xu, H. Gu and J. Lian, *Adv Mater*, 2009, **21**, 217.
- 12 Z. Zhelev, H. Ohba and R. Bakalova, *J Am Chem Soc*. 2006, **128**, 6324;
- 13 C. Zhang, C. Li, C. Peng, R. Chai, S. Huang and D. Yang, *Chem Eur J*, 2010, **16**, 5672.
- 14 Y. Kobayashi, *J. Leukoc. Biol*. 2010, **88**, 1157.
- 15 L. A. Perrone, J. A. Belser, D. A. Wadford, J. M. Katz and T. M. Tumpey, *J. Infect. Dis*, 2013, **207**, 1576.
- 16 R. A. Roberts, D. L. Laskin, C. V. Smith, F. M. Robertson, E. M. Allen, J. A. Doorn and W. Slikker, *Toxicol. Sci.*, 2009, **112**, 4.